

Antoni Sawicki

The Modelling of Electric Arc with Stochastic Disturbances Part. 2. Simulating the Impact of Randomly Disturbed Models of Electric Arc on the Welding System and Power Supply Network

Abstract: The article contains the justification for undertaking a study concerning the impact of random disturbances of AC arc on power supply systems of welding machines. In addition, the paper describes principles governing the development of arc macromodels using controlled voltage and current sources. Particular attention is paid to the magnitude of harmonic distortions of the THD+N signal (helpful in the quantitative assessment of the impact of randomly disturbed non-linear devices on supply networks). The article also presents macromodels of arcs corresponding to selected mathematical models, results of the simulated operation of these macromodels in the form of dynamic current-voltage characteristics and corresponding sets of measurement values of harmonic distortions of voltage. The study discussed in the article involved the investigation of processes occurring in the power supply system of the welding transformer loaded with randomly disturbed electric arc (found to be effective in the filtering of higher harmonics).

Keywords: electric arc, welding system, stochastic disturbances

DOI: 10.17729/ebs.2023.3/7

Introduction

Electric arc in operational tests and physical experiments is always accompanied by stochastic disturbances, whose intensity and frequency range depend on the design and operating conditions of electrotechnical equipment. The obtainment of high precision in the modelling of physical processes by mathematical models and macromodels in simulation programmes requires taking into account random disturbances [1, 2]. Random disturbances can be formed both in near-electrode areas and in the plasma column. Publication [3] presents three variants concerning the modelling of disturbances in the column depending on types of deterministic mathematical models. The generator of noise may disturb geometrical dimensions of the column, constant parameters of mathematical models or the loading of the circuit by electric arc. In the above-named publication, cases of low and high-current arcs are discussed separately. The high effectiveness of simulation tests of

stochastically disturbed arcs can be useful in the assessment of the operation of diagnostic and automatic control systems.

In welding engineering, direct current is used more frequently than alternating one. Direct current provides higher stability of burning arcs and reduces the spatter of liquid metals. As a result, the quality and strength of joints are higher.

The use of alternating current is preferable during the welding of magnetic materials as it is possible to obtain higher arc stability. Alternating current is also used to weld aluminium as it enables the disintegration of undesired oxide layers. In addition, because of lower arc temperature and deeper metal penetration, alternating current enables the welding of thick plates. Alternating current used in the process does not need to be sinusoidal; it can also have basic frequency different from 50 Hz (mains frequency). However, the application of simple and cheap power supply sources or high power sources involves the use of variants with single-phase welding transformers enabling

the obtainment of sinusoidal current arc [4]. Alternating current arcs are also used in some types of plasmatrons and furnaces [5, 6]. Variants in which two or three arcs are generated involve the use of three-phase transformers.

The steeply declining current-voltage characteristic of the current source is obtained by using a transformer provided with the core of increased scattering or featuring an additional choking coil. Such sources are reliable and cheap. In comparison with regular transformers, the disadvantage of the aforesaid devices is high current drawn from the power supply network in spite of the same value of load active power. The reduction of current requires the application of special capacitors enabling the compensation of inductive component. Problems are posed by significant changes of the component as its value is low in the no-load state and high during the welding process. Sometimes, the change of welding machine current settings is coupled with the switching of capacitors on the mains side. Another solution involves the use of the transformer developed by A.P. Budyonny [7], with the core characterised by a complex and branched design (enabling the saturation of the core in the no-load state).

Remarks concerning the modelling and testing of circuits with randomly disturbed electric arc

This part of the article discusses schematic diagrams of arc macromodels constituting modifications of figures presented in publication [8]. These diagrams make it possible to include random disturbances in macromodels containing controlled voltage or current sources as the load. The state variable of mathematical models was conductance or the geometric radius of the arc column.

When building macromodels of electric arcs it is necessary to take into account principles governing connections of (controlled and not-controlled) ideal sources of electric energy:

- a) voltage sources of different values must not be connected in parallel,
- b) current sources of different values must not be connected in series,
- c) result of the parallel connection of the ideal voltage source and the ideal current source is the ideal voltage source, where the current source does not affect resultant voltage and, as such, is ignored,

- d) result of the serial connection of the ideal current source and the ideal voltage source is the ideal current source, where the voltage source does not affect resultant current and, as such, is ignored.

The above-presented principles result from the properties of the sources. The ideal voltage source is characterised by internal impedance $Z = 0 \Omega$, whereas the ideal current source is characterised by internal impedance $Z = \infty \Omega$.

Actual voltage and current sources have, additionally included, appropriate internal impedance. In the aforesaid situation, such sources can be connected nearly in any way. In order to create arc macromodels using various controlled ideal sources it is necessary to modify some of them so that they could become actual sources:

- a) in order to create the parallel connection of various ideal voltage sources it is possible to transform them into actual voltage sources by connecting low-value resistance to each of them in series,
- b) in order to create the serial connection of various ideal current sources it is possible to transform them into actual current sources by connecting high-value resistance to them in parallel,
- c) in the parallel connection of the ideal voltage source and the ideal current source it is possible to transform the voltage source into the actual voltage source by connecting low-value resistance to the former in series,
- d) in the serial connection of the ideal voltage source and the ideal current source it is possible to transform the current source into the actual current source by connecting high-value resistance to the former in series.

The above-presented imperfection of power supply sources does not need to be high to affect the accuracy of the modelling of processes in circuits with electric arc. As a result, in certain cases it is possible to improve the stability of numerical calculations. Using only resistance or only conductance simplifies simulations as it eliminates the need for the adjustment of initial conditions of the conservative element to the initial parameters of the source.

The obtainment of the high accuracy of the modelling of short (low-voltage) arcs requires taking into account the sum of near-electrode voltage drops. In such a case, the fraction of the sum in relation to the resultant arc voltage could be high.

During the modelling of long (high-current) arcs, the sum of near-electrode voltage drops is often ignored as its fraction may be low in relation to the resultant arc voltage. Because of the shape of current-voltage characteristics of the near-electrode area [3], the latter is often modelled using the ideal non-linear voltage source. Afterwards, the area is connected in series to the non-linear resistance of the arc plasma column.

In order to assess the effect of non-linear receivers on power supply networks it is often necessary to use the coefficient of the harmonic distortion of the signal [9, 10]. If the coefficient contains deterministic harmonics, it can be expressed using the following formula:

$$THDf_n = \frac{\sqrt{\sum_{i=2}^n V_i^2}}{V_1} 100\% \quad (1)$$

The total harmonic distortions of the signal along with noise can be expressed using the following formula:

$$THDf_n + N = \frac{\sqrt{\sum_{i=2}^n V_i^2 + V_{noise}^2}}{V_1} 100\% \quad (2)$$

where $THDf_n + N > THDf_n$, V_i – root-mean-square values of harmonics, V_1 – root-mean-square value of the primary harmonic and V_{noise} – root-mean-square value of the random component.

Often in measurements, another definition of the harmonic distortion of the signal containing deterministic components is used:

$$THDr_n = \frac{\sqrt{\sum_{i=2}^n V_i^2}}{V_{total}} 100\% \quad (3)$$

Total harmonic distortions of the signal along with noise can also be expressed using the following formula:

$$THDr_n + N = \frac{\sqrt{\sum_{i=2}^n V_i^2 + V_{noise}^2}}{V_{total}} 100\% \quad (4)$$

where $THDr_n + N > THDr_n$, V_{total} – root-mean-square value of all harmonics (except for the constant component). The correlation between coefficients $THDf$ and $THDr$ is the following:

$$THDr_n = \frac{THDf_n}{\sqrt{1 + THDf_n^2}} \quad (5)$$

Sometimes, values of the harmonic distortion of the signal are expressed in decibels.

The EN 50160 standard, concerning low (nN) and medium voltage (sN) having a nominal frequency of 50 Hz, sets the limit of total voltage harmonics at a level of 8% as well as limits of individual voltage harmonics up to the 40-th harmonic. The width of the time window related to the analysis of DFT is also specified and amounts to 200 ms; the frequency distribution amounts to 5 Hz. Related standards also recommend the averaging of determined Ah values within a very short (3 s), short (10 min) and long (2 hours) measurement time. In cases of numerical simulations, such an approach requires the use of a fast computer and the assumption of a long calculation time.

In measurements and numerical calculations, the reduction of obtained values of harmonic signal distortions is affected by the limit frequency of applied low-pass filters.

In spite of the fact that, in the remainder of the article, the above-presented coefficients are used to assess the effect of electric arcs on their powering systems, similar tests can be performed in networks powering power electronic transducers with arcs or other loads.

Macromodels of electric arcs with randomly disturbed geometrical parameters of the column

The Mayr-Voronin and Cassie-Voronin mathematical models of electric arc enable taking into consideration the effect of geometrical parameters of the plasma column on the value of the resistance load affecting the circuit [3, 11]. Random disturbances ξ of these parameters may significantly affect voltage and current waveforms in time. Schematic diagrams of such macromodels powered by the source of sinusoidal current are presented in Figure 1. The diagrams include the possibility of using mathematical models of the arc column in the differential or integral form, using conductance as the state variable. The foregoing resulted in the application of controlled voltage or current sources. The diagrams also include the possibility of introducing random disturbances of near-electrode voltage drops using the macromodel of the controlled voltage source connected in series.

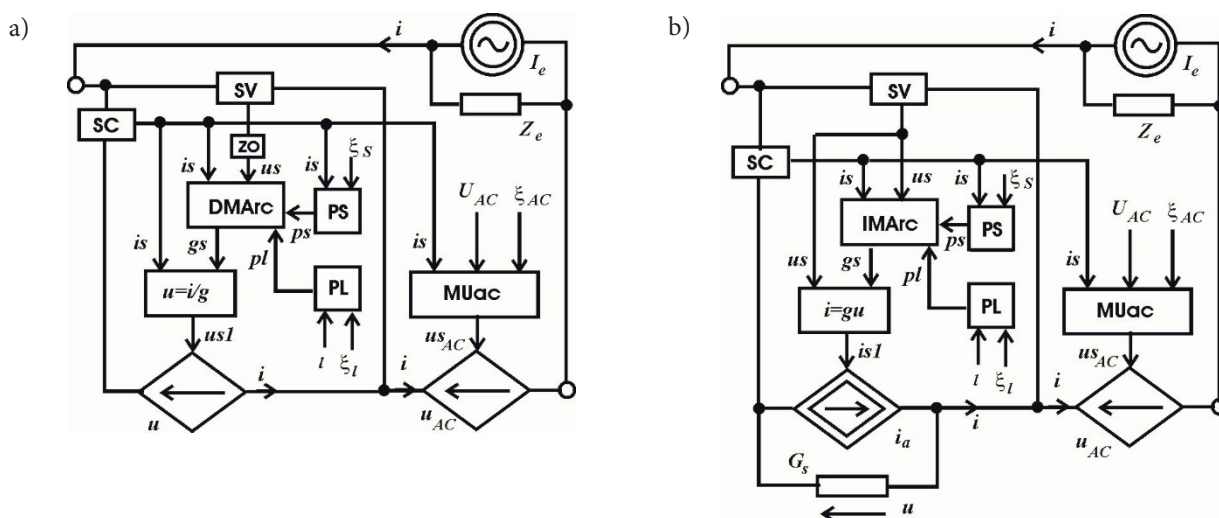


Fig. 1. Schematic diagrams of electric circuits composed of the power supply source and macromodels connected in series and representing quasi-homogenous areas of electric arc described using the Mayr-Voronin or Cassie-Voronin model with deterministically preset parameters randomly disturbed by the column length and sums of disturbed near-electrode voltage drops expressed by means of formulas presented in article [3]: a) described using differential equation (30) or (43) and b) described using integral equation (39) or (48) (SC – current sensor, SV – voltage sensor, DMArc – block performing the differential equation, IMArc – block performing the integral equation, MUac – block performing equation (26) or (27), PL – block performing equation (54), PS – block performing equations (52) and (55) and zo – unit protecting against division by zero)

Macromodels of arc, in which the cross-sectional area of column S is constant and relatively low or changes along with current within a small range should best be developed on the basis of Mayr-Voronin mathematical models. Because of the fact that the notion of low-current arc is relative (depending, among other things, on the nominal current of a given device), the arc column radius can be determined using formula (51) or (52) presented in article [3], with root-mean-square current.

Figures 2 and 3 present dynamic characteristics resulting from simulations of low-current arcs with randomly disturbed column length ξ_l and powered

by the source of sinusoidal current having an amplitude of 5 A and a frequency of 50 Hz. The descriptions under the figures contain values of such parameters as U_{DC} – average value, U_{RMS} – root-mean-square value and values of coefficients of harmonic distortions of voltage THD .

The macromodels of arcs, in which the value of the cross-sectional area of column S is relatively high and changes within a wide range along with high current should best be developed on the basis of the Cassie-Voronin mathematical model. The arc column radius can be determined using

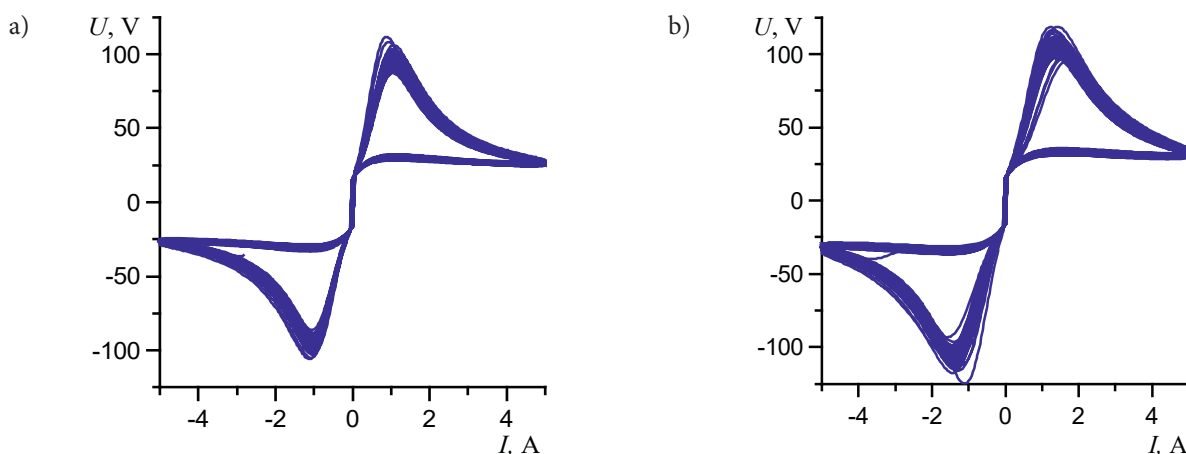


Fig. 2. Dynamic characteristics of electric arcs described in article [3] using the Mayr-Voronin model with the randomly disturbed column length ($\sigma_{0M} = 800 \text{ S/m}$, $l_0 = 4 \cdot 10^{-3} \text{ m}$, $S_0 = 12 \cdot 10^{-6} \text{ m}^2$, $\xi_l = 0.005$, $U_{AK} = 16 \text{ V}$): a) using equation (30) and the macromodel of arc presented in Figure 1a ($p_s = 1 \cdot 10^6 \text{ W/m}^2$, $q_{0M} = 0.5 \cdot 10^6 \text{ J/m}^3$, $U_{DC} = 0.5639 \text{ V}$, $U_{RMS} = 37.89 \text{ V}$, $THDf+N = 81.77\%$ and $THDr+N = 63.29\%$) and b) using equation (39) and the macromodel of arc presented in Figure 1b ($p_s = 1.5 \cdot 10^6 \text{ W/m}^2$, $q_{0M} = 1 \cdot 10^6 \text{ J/m}^3$, $U_{DC} = -1.32 \text{ V}$, $U_{RMS} = 70.86 \text{ V}$, $THDf+N = 74.5\%$ and $THDr+N = 59.73\%$)

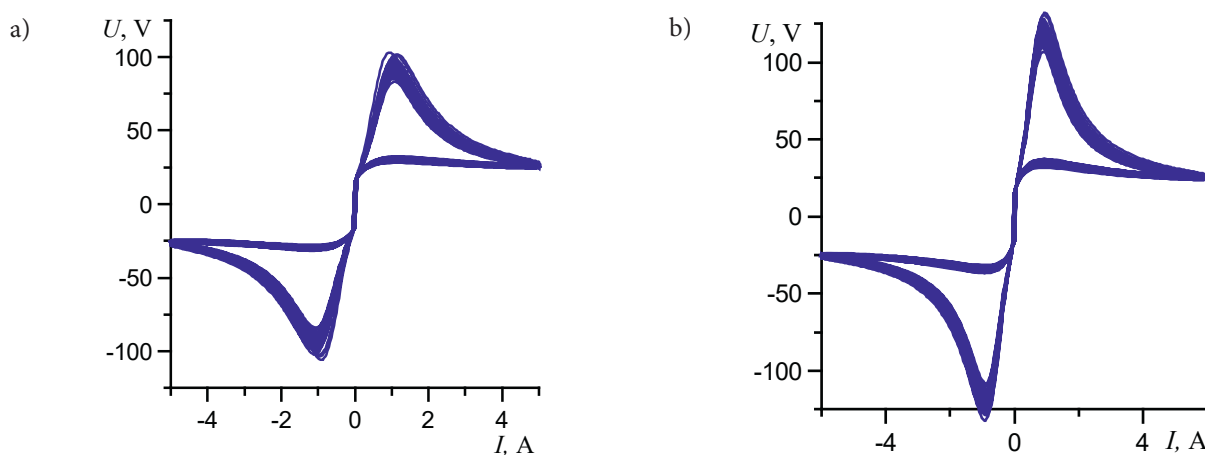


Fig. 3. Dynamic characteristics of electric arcs described using the Mayr-Voronin model with the randomly disturbed column length and expressed using equation (39) in article [3] ($q_{0M} = 0.5 \cdot 10^6 \text{ J/m}^3$, $\sigma_{0M} = 800 \text{ S/m}$, $S_0 = 12 \cdot 10^{-6} \text{ m}^2$, $\xi_1 = 0.005$): a) using the macromodel of arc presented in Figure 1a ($p_v = 1 \cdot 10^9 \text{ W/m}^3$, $l_0 = 4 \cdot 10^{-3} \text{ m}$, $U_{DC} = -0.5481 \text{ V}$, $U_{RMS} = 37.15 \text{ V}$, $THDf+N = 80.42\%$ and $THDr+N = 62.66\%$) and b) using the macromodel of arc presented in Figure 1b ($p_v = 1.5 \cdot 10^9 \text{ W/m}^3$, $l_0 = 3 \cdot 10^{-3} \text{ m}$, $U_{DC} = -0.5585 \text{ V}$, $U_{RMS} = 39.19 \text{ V}$, $THDf+N = 95.81\%$ and $THDr+N = 69.17\%$)

formula (51) or (52), described in article [3], with the variable momentary value of current.

Figures 4 and 5 present dynamic current-voltage characteristics resulting from simulations of high-current arcs with randomly disturbed column length ξ_i and powered by the source of sinusoidal current having a frequency of 50 Hz.

Macromodels of electric arcs with randomly disturbed parameters of mathematical models

In Mayr and Cassie mathematical models of the electric arc column it is assumed that parameters are constant. In fact, parameters of plasma, waveforms of electric parameters in time and dynamic

characteristics of arc undergo random changes. Because of the foregoing, parameters of deterministic models should also change randomly. In order to take such changes into consideration it is necessary to introduce disturbances of at least one of parameters (P_a). Schematic diagrams of such macromodels powered by the source of sinusoidal current are presented in Figure 6. The diagrams include the possibility of using mathematical models in the differential or integral form, using conductance as the state variable. The foregoing resulted in the application of controlled voltage or current sources. The diagrams also include the possibility of introducing random disturbances of near-electrode voltage drops using the macromodel of the controlled voltage source connected in series. In article

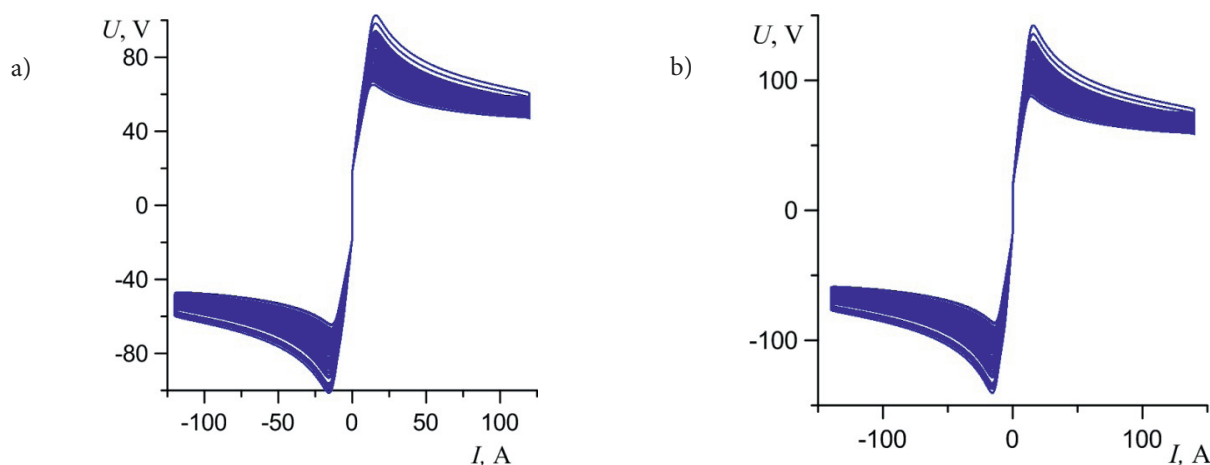


Fig. 4. Dynamic characteristics of electric arcs described in article [3] using the Cassie-Voronin model with the randomly disturbed geometrical parameters of the column ($\sigma_{0C} = 800 \text{ S/m}$, $q_v = 2.5 \cdot 10^4 \text{ J/m}^3$, $l_0 = 6 \cdot 10^{-3} \text{ m}$, $I_0 = 10 \text{ A}$, $k_r = 0.1$, $= 0.6$, $K_r = 0.135$, $r_{0M} = 6 \cdot 10^{-2} \text{ m}$, $\xi_1 = 0.05$, $f = 50 \text{ Hz}$): a) using equation (43) and the macromodel of arc presented in Figure 1a ($p_s = 1 \cdot 10^6 \text{ W/m}^2$, $q_{0C} = 2 \cdot 10^5 \text{ J/m}^3$, $U_{AK} = 18 \text{ V}$, $I_m = 120 \text{ A}$, $U_{DC} = 0.961 \text{ V}$, $U_{RMS} = 56.99 \text{ V}$, $THDf+N = 58.77\%$ and $THDr+N = 50.65\%$) and b) using equation (48) and the macromodel of arc presented in Figure 1b ($p_s = 1.2 \cdot 10^6 \text{ W/m}^2$, $q_{0C} = 3 \cdot 10^5 \text{ J/m}^3$, $U_{AK} = 16 \text{ V}$, $I_m = 140 \text{ A}$, $U_{DC} = 1.347 \text{ V}$, $U_{RMS} = 73.34 \text{ V}$, $THDf+N = 61.52\%$ and $THDr+N = 52.38\%$)

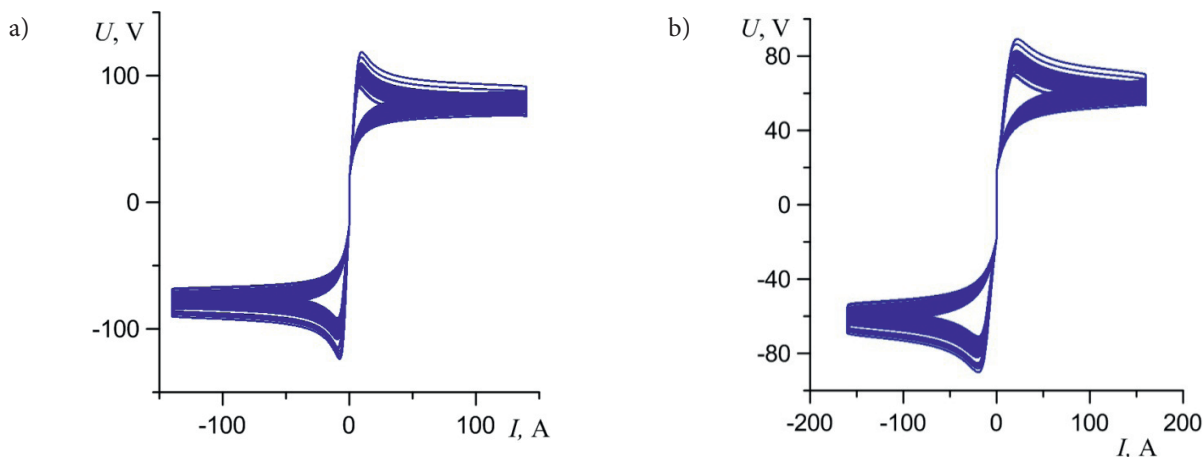


Fig. 5. Dynamic characteristics of electric arcs described in article [3] using the Cassie-Voronin model with the randomly disturbed geometrical parameters of the column ($p_V = 50 \cdot 10^6 \text{ W/m}^3$, $q_{0C} = 16 \cdot 10^6 \text{ J/m}^3$, $\sigma_{0C} = 800 \text{ S/m}$, $l_0 = 6 \cdot 10^{-3} \text{ m}$, $k_r = 0.1$, $n = 0.6$, $r_{0M} = 6 \cdot 10^{-2} \text{ m}$, $\xi_l = 0.005$, $U_{AK} = 16 \text{ V}$, $I_0 = 10 \text{ A}$, $f = 50 \text{ Hz}$): a) using equation (48) and the macromodel of arc presented in Figure 1a ($q_v = 1 \cdot 10^4 \text{ J/m}^3$, $K_r = 0.135$, $I_m = 140 \text{ A}$; $U_{DC} = 1.429 \text{ V}$, $U_{RMS} = 74.54 \text{ V}$, $THDf+N = 45.01\%$ and $THDr+N = 41.03\%$) and b) using equation (48) and the macromodel of arc presented in Figure 1b ($q_v = 2 \cdot 10^4 \text{ J/m}^3$, $K_r = 0.138$, $I_m = 160 \text{ A}$, $U_{DC} = 1.051 \text{ V}$, $U_{RMS} = 58.06 \text{ V}$, $THDf+N = 44.27\%$ and $THDr+N = 40.47\%$)

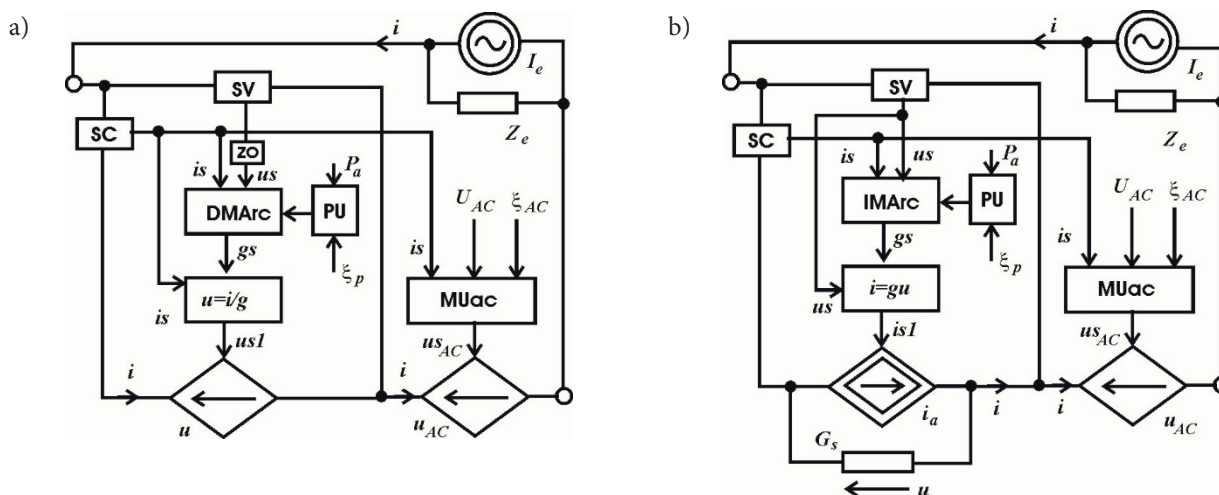


Fig. 6. Schematic diagrams of electric circuits composed of the power supply source and macromodels connected in series and representing quasi-homogenous areas of electric arc described using the Mayr-Voronin or Cassie-Voronin model and the model of the sum of disturbed near-electrode voltage drops described in article [3]: (SC – current sensor, SV – voltage sensor, DMARc – block performing the differential equations (58) or (60), IMARc – block performing equations (6) or (7) presented in this article, MUAc – block performing equation (26) or (27), PU – block performing changes of the parameter described using correlation (63) or (64): a) using the controlled voltage source and b) using the controlled current source

[3], formulas (58) and (60) were used to describe the Mayr and Cassie mathematical models of the column in the differential form. In turn, the integral forms of column models were the following:

- Mayr model:

$$g = g_0 \exp\left(\frac{1}{\theta_M} \int_0^t \left(\frac{i^2}{gP_M} - 1\right) d\tau\right) \quad (6)$$

- Cassie model:

$$g = g_0 \exp\left(\frac{1}{2\theta_C} \int_0^t \left(\frac{i^2}{gU_C^2} - 1\right) d\tau\right) \quad (7)$$

The diagrams also include the possibility of introducing random disturbances of near-electrode

voltage drops using the controlled voltage source connected in series.

Figure 7 presents the dynamic current-voltage characteristic of arc described using the Mayr model, whereas Figure 8 presents the dynamic current-voltage characteristic of arc described using the Cassie model.

Some publications [2, 5, and 12] describe mathematical models of arc, where the electric state variable (conductance or resistance) is replaced by the geometrical radius. The variable diameter of the column indicates the particular usability of such models in the representation (modelling) of

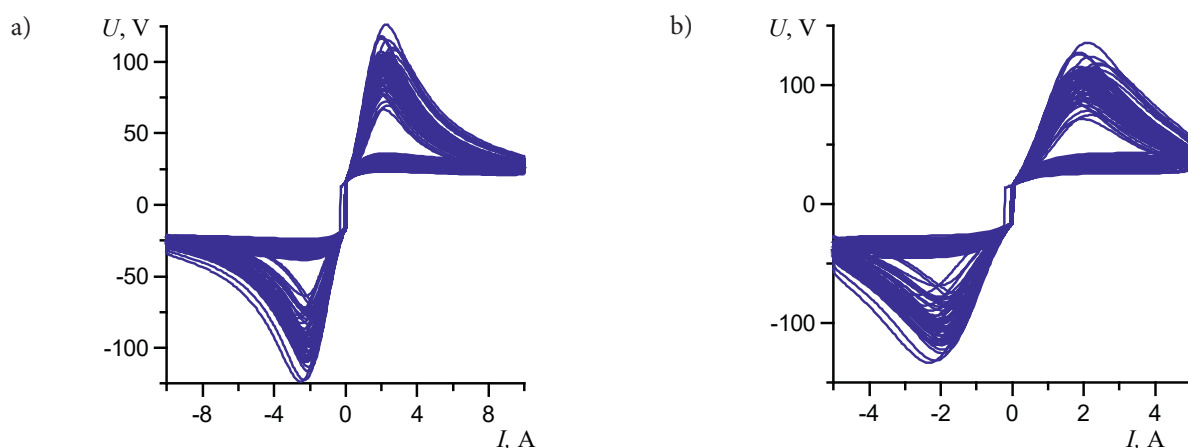


Fig. 7. Dynamic characteristics of electric arcs described using the Mayr model with randomly disturbed power P_M ($P_M = 100$ W, $\xi_p = 0.005$, $U_{AK} = 16$ V, $f = 50$ Hz): a) using the macromodel of arc presented in Figure 6a ($\theta_M = 5 \cdot 10^{-4}$ s, $I_m = 10$ A, $U_{DC} = 1.778$ V, $U_{RMS} = 35.66$ V, $THDf+N = 79.89\%$ and $THDr+N = 62.3\%$) and b) using the macromodel of arc presented in Figure 6b ($\theta_M = 2 \cdot 10^{-3}$ s, $I_m = 5$ A, $U_{DC} = 2.969$ V, $U_{RMS} = 47.18$ V, $THDf+N = 59.18\%$ and $THDr+N = 50.8\%$)

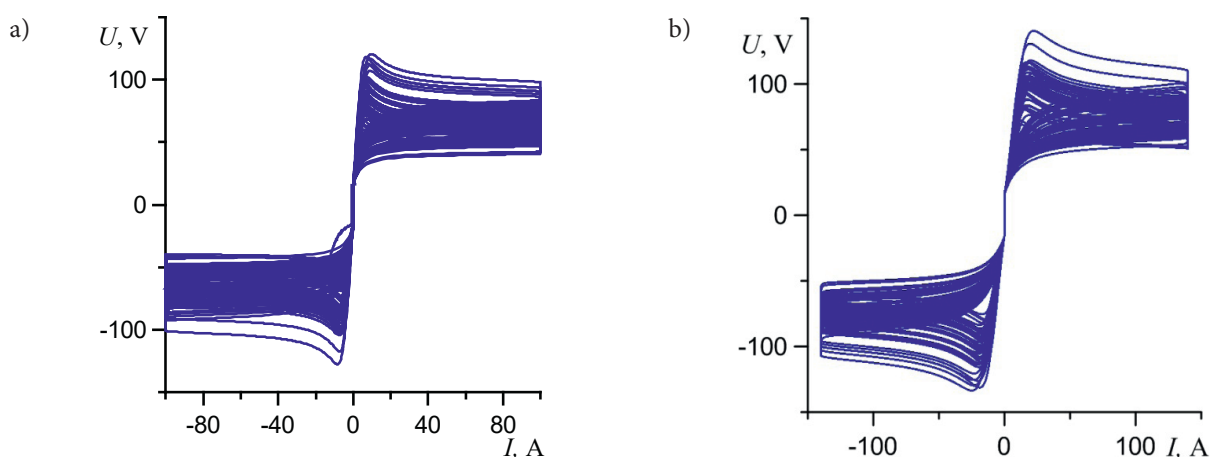


Fig. 8. Dynamic characteristics of electric arcs described in article [3] using the Cassie model with randomly disturbed voltage U_C ($U_{AK} = 16$ V, $f = 50$ Hz): a) using equation (60) presented in article [3] and the macromodel of arc presented in Figure 6a ($U_C = 50$ V, $\theta_C = 1 \cdot 10^{-4}$ s, $\xi_p = 0.005$, $I_m = 100$ A, $U_{DC} = 3.663$ V, $U_{RMS} = 58.58$ V, $THDf+N = 46.55\%$ and $THDr+N = 42.06\%$) and b) z using equation (7) and the macromodel of arc presented in Figure 6b ($U_C = 60$ V, $\theta_C = 2 \cdot 10^{-4}$ s, $\xi = 0.004$, $I_m = 140$ A, $U_{DC} = 3.659$ V, $U_{RMS} = 69.09$ V, $THDf+N = 45.26\%$ and $THDr+N = 41.14\%$)

electric properties of high-current arcs. In article [3], formula (66) was used to describe the model of the column in the differential form. In turn, the integral part of the column model is the following:

$$g = \frac{r_a^{m+2}}{k_3} = \frac{1}{k_3} \left\{ r_{a0} \exp \left[\int_0^t \left(\frac{k_3}{k_2} \frac{i^2}{r_a^{m+4}} - \frac{k_1}{k_2} r_a^{n-2} \right) d\tau \right] \right\}^{m+2} \quad (8)$$

In order to take into consideration random changes of voltage waveforms it was necessary to introduce disturbances of one of the parameters. In the case under discussion this was parameter k_3 .

Schematic diagrams of macromodels of arc powered by the source of sinusoidal current are presented in Figure 9. The diagrams include the possibility of applying mathematical models in the differential or integral form. The models could

be transformed to enable the use of conductance as the state variable. The foregoing resulted in the application of controlled voltage or current sources. The diagrams also include the possibility of introducing random disturbances of near-electrode voltage drops using the controlled voltage source connected in series. The results of the simulation of processes in circuits with the above-named arc models are presented in Figure 10.

Macromodels of randomly disturbed loads including electric arcs

The column of arc constitutes a non-linear resistant element. Random disturbances generated in the arc column can be presented in the form of a branch of a circuit of serial structure or as the parallel connection of two elements. One of these

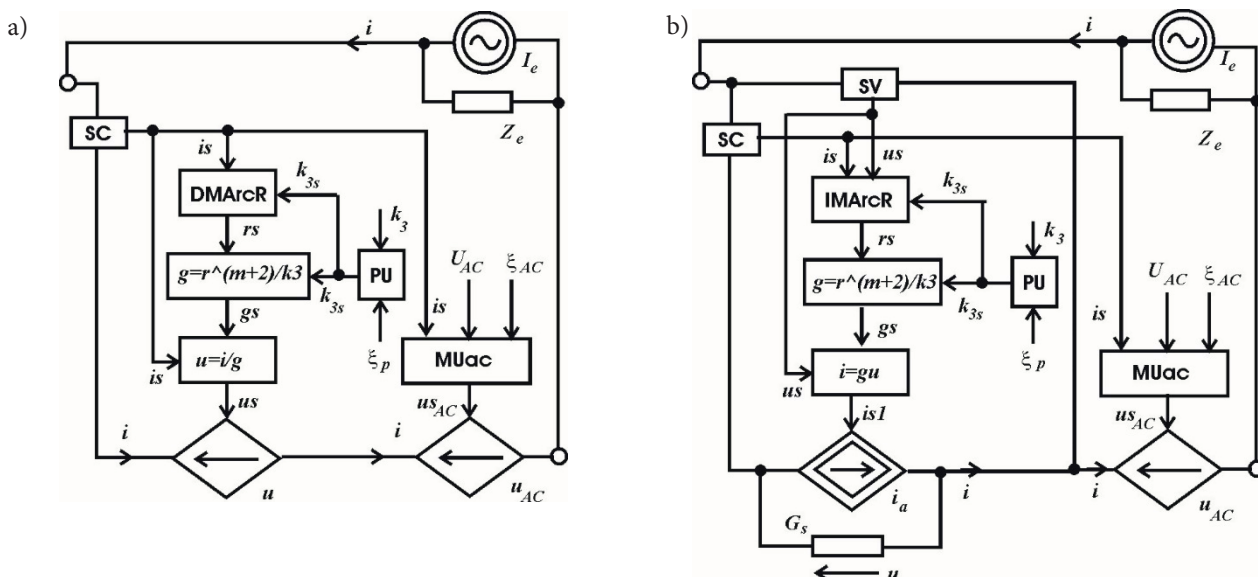


Fig. 9. Schematic diagrams of electric circuits composed of the power supply source and macromodels connected in series and representing quasi-homogenous areas of electric arc composed of the model of the column with the radial state variable and the model of the sum of disturbed near-electrode voltage drops: a) described using differential equation (66) in article [3] and b) described using integral equation (8) in this publication (SC – current sensor, SV – voltage sensor, DMArc – block performing the differential equation, IMArc – block performing the integral equation, MUac – block performing equation (26) or (27) and PU – block performing equation (68) in article [3])

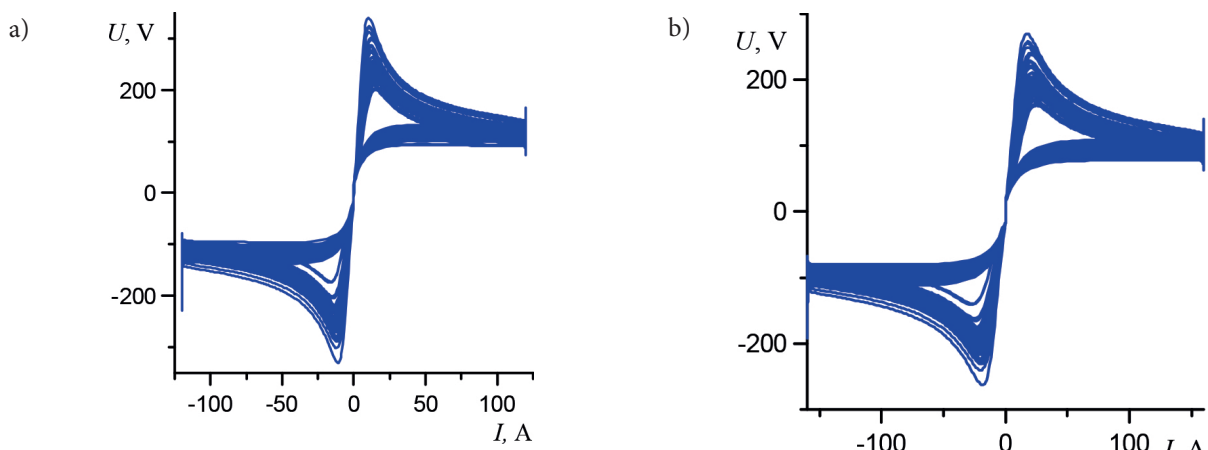


Fig. 10. Dynamic characteristics of electric arcs described using the model with the radius as the state variable and with randomly disturbed parameter k_3 ($k_2 = 2, k_3 = 12.5, m = 1, n = 2, \xi_p = 0.005, U_{AK} = 16 \text{ V}, I_m = 120 \text{ A}, f = 50 \text{ Hz}$): a) using equation (66) presented in article [3] and the macromodel of arc presented in Figure 9a ($k_1 = 2000, r_0 = 20 \cdot 10^{-3} \text{ m}, I_m = 120 \text{ A}, U_{DC} = 3.863 \text{ V}, U_{RMS} = 125.3 \text{ V}, THD_{f+N} = 58.75\%$ and $THD_{r+N} = 50.61\%$) and b) using equation (8) and the macromodel of arc presented in Figure 9b ($k_1 = 1600, r_0 = 10 \cdot 10^{-3} \text{ m}, I_m = 160 \text{ A}, U_{DC} = 3.205 \text{ V}, U_{RMS} = 106 \text{ V}, THD_{f+N} = 56.64\%$ and $THD_{r+N} = 49.23\%$)

elements is described using the deterministic model of arc, whereas the second element is the source of random disturbances. The arc column model can be expressed using the form of the differential or integral equation. In the former case, the model corresponds to the voltage source, whereas in the latter case the model corresponds to the current source (Fig. 11). These sources are connected in series to two voltage sources. One enables the introduction of column disturbances, whereas the other one represents the sum of near-electrode voltage drops.

Figure 12 presents dynamic current-voltage characteristics of arc, the column of which is described using the Mayr model. The results of simulation were obtained using the macromodels presented in Figure 11. The macromodels were used also to simulate processes in the circuit with arc, the column of which was described using the Cassie model. The results of the simulation of the above-named model are presented in Figure 13.

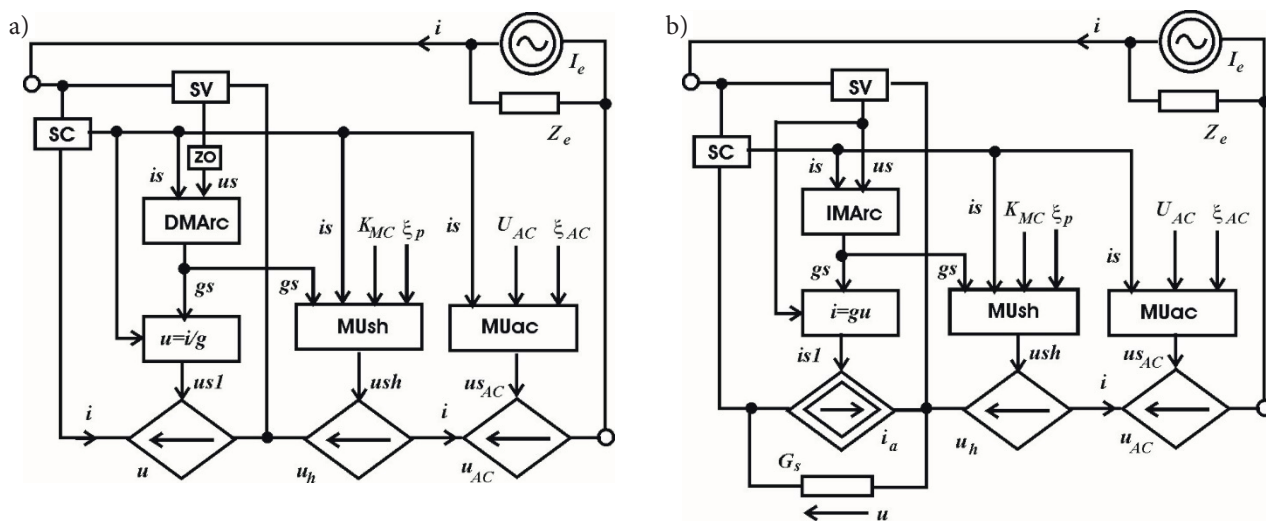


Fig. 11. Schematic diagrams of electric circuits composed of the power supply source and macromodels connected in series and representing quasi-homogenous areas of electric arc and the model of the sum of disturbed near-electrode voltage drops described using formulas presented in article [3] (SC – current sensor, SV – voltage sensor, DMArc – block performing equation (58) or (60), IMArc – block performing equation (6) or (7), MUac – block performing equation (26) or (27): a) using macromodels including three controlled voltage sources and b) using the column macromodel including the controlled current source and macromodels including two controlled voltage sources

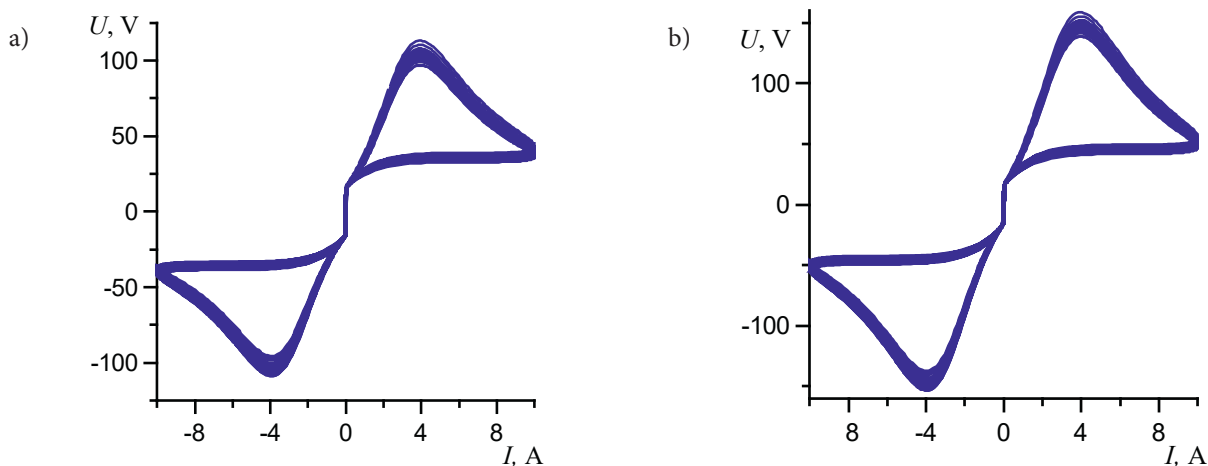


Fig. 12. Dynamic characteristics of electric arcs described using the Mayr model with randomly disturbed parameter ($\theta_C = 1 \cdot 10^{-3}$ s, $K_{Mu} = 2$, $\xi_p = 0.005$, $U_{AK} = 16$ V, $I_m = 10$ A, $f = 50$ Hz): a) using formulas (58) and (80) and the macromodel of arc presented in Figure 11a ($P_M = 200$ W, $U_{DC} = -1.075$ V, $U_{RMS} = 51.96$ V, $THD_{f+N} = 58.91\%$ and $THD_{r+N} = 50.74\%$) and b) using formulas (6) and (80) the macromodel of arc presented in Figure 11b ($P_M = 300$ W, $U_{DC} = -1.32$ V, $U_{RMS} = 70.86$ V, $THD_{f+N} = 60.56\%$ and $THD_{r+N} = 51.76\%$)

Simulation of the welding system effect on the power supply network

The values of *THD* voltage coefficients in the system with electric arc were identified using simulation. Because their wavelength in time was an irregular function, the aforesaid function was subjected to averaging. As regards voltage between the electrodes, the values of *THD* were nearly ten-fold higher than those allowed in power supply networks [13]. The foregoing could affect the functioning of control and measurement systems in the structure of power transformers [14] and welding transformers as well as to lead to an increase in

losses in the transformer core. In order to investigate the effect of welding systems on the power supply network it was necessary to take into consideration transformer attenuation. Figure 14 presents the schematic diagram of a measurement system. The graphic results concerning the simulation of the system are presented in Figures 15 and 16, whereas numerical values are presented in Table 1. The values of *THD* voltage coefficients on the primary side of the transformer were significantly lower than values permissible in low-voltage networks.

Figure 16a reveals that the spectral function of power density [3] had a significant extremum in

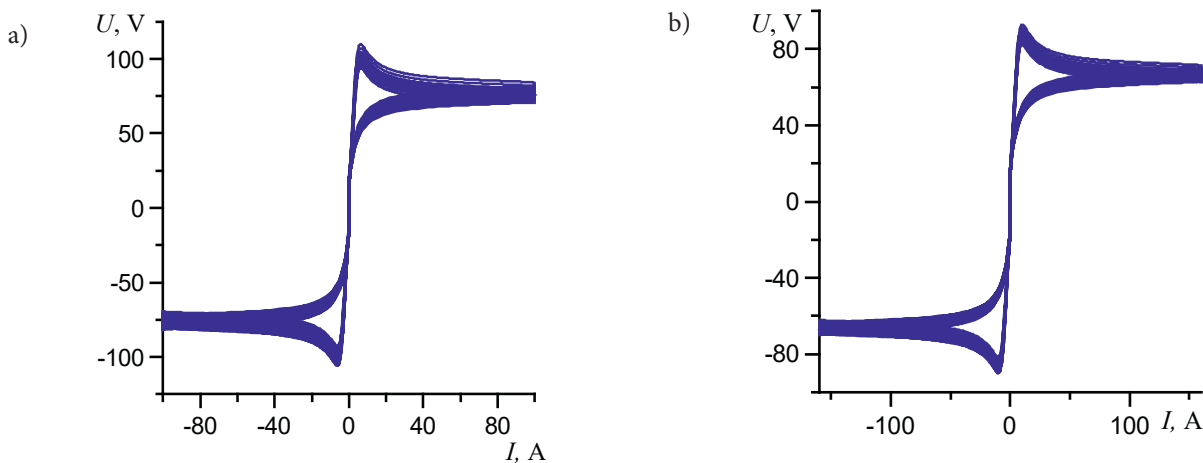


Fig. 13. Dynamic characteristics of electric arcs described using the Cassie model with randomly disturbed parameter ($U_C = 60$ V, $\theta_C = 1 \cdot 10^{-4}$ s, $\xi_p = 0.005$, $U_{AK} = 16$ V, $f = 50$ Hz): a) using formulas (60) and (80) and the macromodel of arc presented in Figure 11a ($K_{Cu} = 2$, $I_m = 100$ A, $U_{DC} = -1.605$ V, $U_{RMS} = 74.6$ V, $THDf+N = 44.73\%$ and $THDr+N = 40.82\%$) and b) using formulas (7) and (82) and the macromodel of arc presented in Figure 11b ($K_{Cu} = 1$, $I_m = 160$ A, $U_{DC} = -1.037$ V, $U_{RMS} = 65.04$ V, $THDf+N = 44.66\%$ and $THDr+N = 40.76\%$)

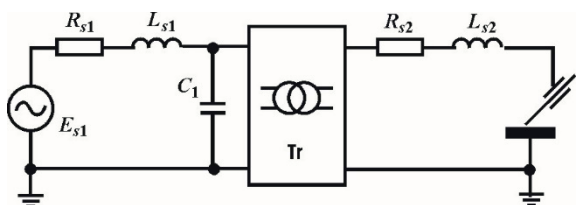


Fig. 14. Schematic diagram of the power supply system of the electric arc-loaded welding transformer ($E_{s1} = 400$ V, $f = 50$ Hz, $R_{s1} = 1 \cdot 10^{-3}$ Ω , $L_{s1} = 2 \cdot 10^{-4}$ H, $R_{s2} = 1 \cdot 10^{-3}$ Ω , $L_{s2} = 1 \cdot 10^{-6}$ H, $C_1 = 5 \cdot 10^{-6}$ F, parameters of the transformer having power $S = 9 \cdot 10^3$ VA and expressed in relative units: $R_1 = 2 \cdot 10^{-2}$, $L_1 = 2 \cdot 10^{-1}$, $R_2 = 3 \cdot 10^{-3}$, $L_2 = 6 \cdot 10^{-3}$, $R_m = 500$, $L_m = 500$)

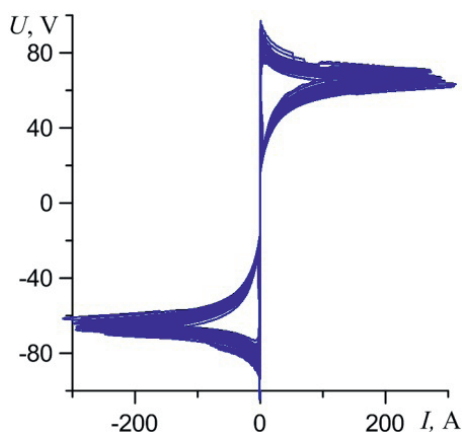


Fig. 15. Dynamic characteristic of electric arc described in article [3] using the Cassie model (60) with randomly disturbed Cassie voltage ($U_C = 50$ V, $\theta_C = 1 \cdot 10^{-4}$ s, $\xi_p = 0.001$, $U_{AK} = 16$ V) and using the power supply system presented in Figure 14

the abscissa having a supply voltage frequency of 50 Hz. There were also smaller extrema, corresponding to odd harmonics, whose values decreased along with increasing frequency. The

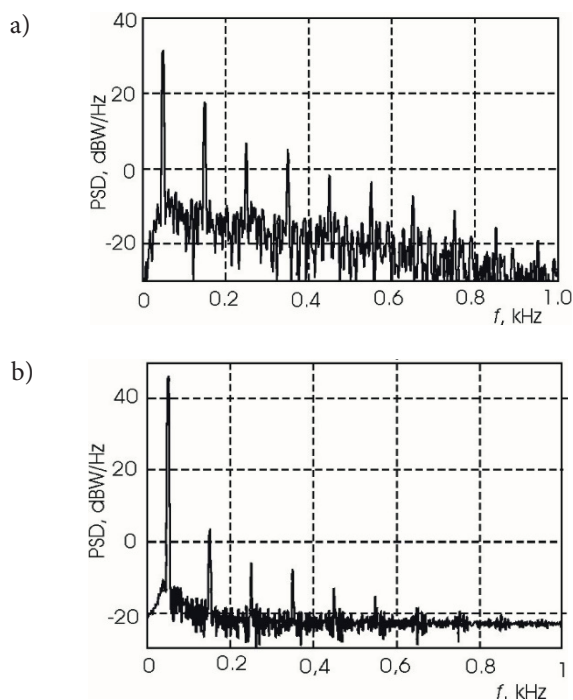


Fig. 16. Spectral function of voltage power density: a) at the out output of the transformer and b) at the input of the welding machine

stochasticity of voltage waveform resulted in the continuity and irregularity of the shape of the spectrum. On the primary side of the transformer it was possible to observe the significantly higher value of the extremum of the primary harmonic and significantly lower values of the remaining harmonics. Very close values of $THDf+N$ and $THDr+N$ resulted from very small differences between them. In accordance with Table 1, the connection of an additional capacitor did not affect already low values of the coefficient of harmonic

Table 1. Values of measurement parameters in the system of the welding transformer with arc (powered by the power supply network)

Measurement parameters	Measurement on the secondary side of the transformer, $C = 5 \cdot 10^{-6}$ F	Measurement on the primary side of the transformer, $C = 5 \cdot 10^{-6}$ F	Measurement on the primary side of the transformer, $C = 0$ F
U_{DC} , V	-0.3494	-0.02351	-0.02185
U_{RMS} , V	64.33	398.7	398.7
THD_f , %	35.43	0.4966	0.495
THD_{f+N} , %	35.76	0.4901	0.4887
THD_{r+N} , %	33.67	0.4901	0.4887

distortions of voltage $THD+N$ in the power supply network.

Conclusions

1. The above-presented simulation tests involved the use of several types of mathematical models of arc described using differential or integral equations of the first order. The introduction of stochastic disturbances was performed using three methods. The results obtained in the tests demonstrated the effectiveness of the macromodels of electric arc developed within the investigation.
2. The significant non-linearity of the dynamic characteristics of arc and additionally introduced randomly disturbed parameters translated into high values of coefficients of harmonic distortions of voltage on the load affecting the supply source of arc. The foregoing led to increased losses in the transformer core and, consequently, to the increased consumption of power from the power supply network.
3. The welding transformed was characterised by inertia and, because of this, it had a filtering effect on generated harmonics and was responsible for low values of coefficients of harmonic distortions in the power supply network.
4. This (i.e. the second) part of the article is only concerned with selected mathematical models of arc and corresponding macromodels with controlled sources connected in series. The simulation of systems of randomly disturbed near-electrode voltage drops was not included. The extended test results will be presented in the subsequent part of the article.

References

- [1] Grabowski D., Walczak J., Klimas M.: Electric arc furnace power quality analysis based on a stochastic arc model. 2018 IEEE International Conference on Environment and Electrical Engineering and 2018 IEEE Industrial and Commercial Power Systems Europe (EEEIC/I&CPS Europe).
- [2] Grabowski D., Walczak J.: Deterministic model of electric arc furnace – a closed form solution. COMPEL – The International Journal for Computation and Mathematics in Electrical and Electronic Engineering, 2013, vol. 32, no. 4, pp. 1428–1436.
- [3] Sawicki A.: Modelowanie łuku elektrycznego z zaburzeniami stochastycznymi. Cz. 1. Odzworowanie zaburzeń stochastycznych w modelach matematycznych łuku elektrycznego. Biuletyn Instytutu Spawalnictwa, 2022, vol. 66, no. 6, pp. 40–52.
- [4] Sawicki A., Świtoń Ł., Sosiński R.: Process Simulation in the AC Welding Arc Circuit Using a Cassie-Mayr Hybrid Model. Supplement to the Welding Journal, 2011, March, pp. 41–44.
- [5] Klimas M., Grabowski D.: Application of shallow neural networks in electric arc furnace modeling. IEEE Transactions on Industry Applications, Sept.–Oct. 2022, vol. 58, no. 5, pp. 6814–6823, DOI: 10.1109/TIA.2022.3180004.
- [6] Sawicki A.: Modelowanie procesów elektrycznych w obwodach plazmotronów łukowych. Cz. 2. Stany dynamiczne w obwodach z plazmotronami jednofazowymi. Biuletyn Instytutu Spawalnictwa, 2022, vol. 66, no. 3, pp. 37–41.
- [7] Budennyj A.P.: Svaročnýj transformator. Patent MPK B23K 9/00, B23K 9/10.
- [8] Sawicki A.: Model Mayra-Pentegowa łuku elektrycznego z wykorzystaniem funkcji wykładniczej do aproksymowania charakterystyk statycznych. Biuletyn Instytutu Spawalnictwa, 2021, vol. 65, no. 1, pp. 32–37.
- [9] Garg Manila, Nijhawan Parag: Mitigation of Power Quality Problems Using DVR in Distribution Network for Welding Load. IOSR Journal of Electrical and Electronics Engineering (IOSR-JEEE) e-ISSN: 2278-1676, p-ISSN: 2320-3331, vol. 10, no. 4, Ver. I (July – Aug. 2015), pp. 106–112.
- [10] Rajpreet Kaur, Shimpy Maheshwari: Comparative Analysis of Total Harmonic Distortion for Welding Load. IJSRSET, 2016, vol. 2, no. 4, pp. 394–396.

- [11] Sawicki A.: Modified Voronin models of electric arc with disturbed geometric dimensions and increased energy dissipation. *Archives of Electrical Engineering*, 2021, vol. 70, no. 1, pp. 89–102.
- [12] Sawicki A.: Mathematical Model of an Electric Arc in Differential and Integral Forms With the Plasma Column Radius as a State Variable. *Acta Energetica*, 2020, no. 2, pp. 57–64.
- [13] Marciniak L.: Implementations of the arc earth faults model in programs PSCAD and Matlab/Simulink. *Przeegląd Elektrotechniczny*, 2012, vol. 9, no. 1, pp. 126–129.
- [14] Marciniak L.: Model of the arc earth-fault for medium voltage networks. *Central European Journal of Engineering*, 2011, vol. 1, no. 6, pp. 168–173.